Available online at www.sciencedirect.com
ScienceDirect
Journal of Power Sources 174 (2007) 394–399
JOURNAL OF POWER SOURCES
www.elsevier.com/locate/jpowsour

Short communication

Fabrication of $LiCoO_2$ cathode powder for thin film battery by aerosol flame deposition

Taewon Lee, Kihyun Cho, Jangwon Oh, Dongwook Shin *

Division of Material Science & Engineering, Hanyang University, 17 Haengdang-dong, Seongdong-gu, Seoul 133-791, Republic of Korea

Available online 28 June 2007

Abstract

Crystalline $LiCoO_2$ nano-particles for thin film battery were synthesized and deposited by aerosol flame deposition (AFD). The aqueous precursor solution of the lithium nitrate and cobalt acetate was atomized with an ultrasonic vibrator and subsequently carried into the central tube of the torch by flowing dry Ar gas. $LiCoO_2$ were formed by oxy-hydrogen flame and deposited on a substrate placed in a heating stage. The deposited soot film composed of nano-sized particles was subsequently consolidated into a dense film by high temperature heat treatment at 500–800 °C for 5 h and characterized by SEM, XRD, and Raman spectroscopy. The crystalline carbonates and oxide were first formed by the deposition and the subsequent heat treatment converted those to $LiCoO_2$. The FWHMs of the XRD peaks were reduced and their intensity increased as the heat treatment temperature increased, which is due to improved crystallinity. When judged from the low enough cation mixing and well-developed layered structure, it is believed that the $LiCoO_2$ film satisfied the quality standard for the real application. SEM measurements showed that $LiCoO_2$ were nano-crystalline structure with the average particle size <70 nm and the particle size increased with the increase of heat treatment temperature. The thickness of thin film $LiCoO_2$ before the consolidation process was about 15 μm and reduced to about 4 μm after sintering.

Keywords: Lithium cobalt oxide; Aerosol flame deposition; Cathode; Micro-battery; Thin film battery

1. Introduction

Rechargeable thin film battery becomes an important power source for various small electronic devices such as micro-electromechanical system, smart card, medical appliances, MEMS devices, and so on. Several thin film micro-rechargeable battery systems were demonstrated successfully [1,2], and its necessity has been grown with the advent of nano-devices and ubiquitous age. To realize the thin film battery, solid electrolyte, cathode, and anode layers have to be developed to the satisfactory level of performance. The fabrication of lithiated intercalation oxides in thin film form is of great interest as a result of their possible use as positive electrode in all-solid-state lithium rechargeable micro-batteries to power microelectronics [3–5]. In the market-oriented viewpoint, the cost for the fabrication of these micro or 'mini' battery cells is not negligible issue and it should be considered from the initial stage of process development. In this study, the new inexpensive deposition method is suggested to prepare $LiCoO_2$ cathode film for 'mini' battery cell fabrication.

$LiCoO_2$ is one of the most extensively used cathode material in rechargeable lithium batteries. The cathode material for thin film battery as well as bulk type battery has been chosen to $LiCoO_2$ without hesitation since its performance as a cathode is excellent and its advantages, such as high operating voltage, high specific capacity, and long cycle-life are evident [7–11]. Fabrication of nano-particle and thin film of $LiCoO_2$ has been extensively investigated and various methods have been suggested such as RF sputtering [11–16], electrostatic spray deposition [17,18], oxidation of metallic Co [19], and pulsed-laser deposition [20–22].

Because of its importance as a cathode material in rechargeable lithium batteries, the electrochemical properties of lithium cobalt oxide have been extensively investigated. The performance of the cathodes materials is affected by several factors such as particle size, crystallinity, and phase purity of the material. It is known that smaller particle size, in micrometer range, produces better cycling stability [6].

In this study, we employed a completely new method to synthesize the oxide cathode, which is called "aerosol flame

* Corresponding author. Tel.: +82 2 2220 0503; fax: +82 2 2299 3851.
E-mail address: dwshin@hanyang.ac.kr (D. Shin).

0378-7753/$ – see front matter © 2007 Elsevier B.V. All rights reserved.
doi:10.1016/j.jpowsour.2007.06.136

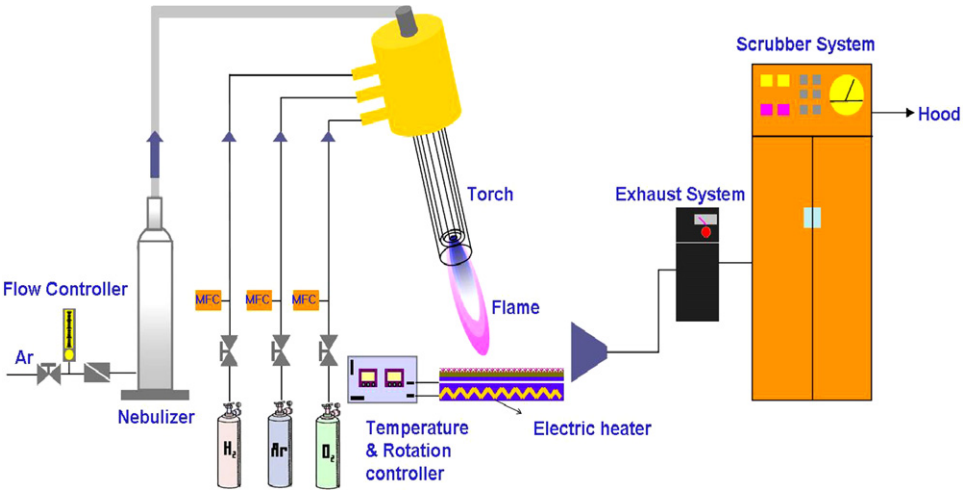

Fig. 1. A schematic diagram of experimental apparatus for the synthesis of $LiCoO_2$ by aerosol flame deposition.

deposition (AFD)" method. Advantages of AFD method are rapid formation of submicron and nano-sized metal oxide particles, simple and low-cost process operating under ambient atmosphere, wide choice of precursors, and good deposition rate for oxide particles.

The nano-particles and film of $LiCoO_2$ was fabricated by supplying precursors into high temperature oxy-hydrogen flame. The deposited soot film composed of nano-particles was subsequently consolidated into solid film by high temperature heat treatment. The whole processes were carried out under normal air atmosphere with only optional control for moisture. The microstructure and crystalline structure of the synthesized powder and films were characterized by SEM, XRD, and Raman spectroscopy.

2. Experiments

The aerosol flame deposition was applied to fabricate soot film of $LiCoO_2$. Fig. 1 schematically shows AFD system. The essential part of the system is the oxy-hydrogen torch (21 mm

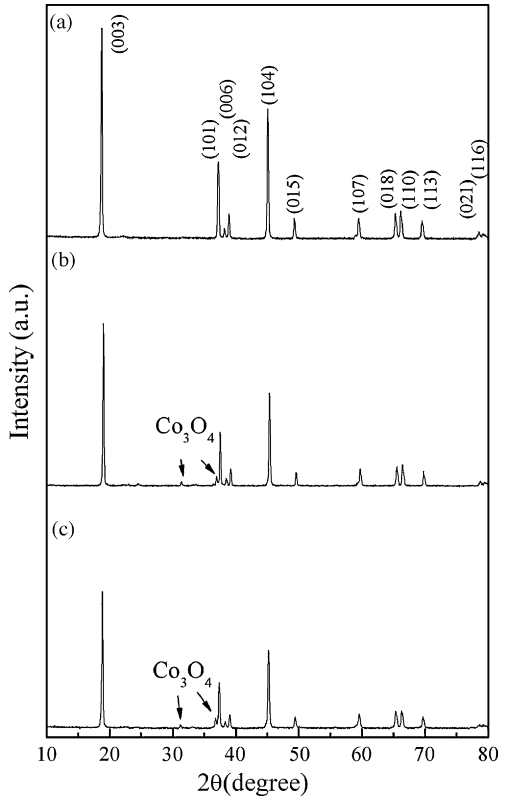

Fig. 2. X-ray diffraction patterns of $LiCoO_2$ powders produced at various ratio between Li and Co and sintered at 700 °C for 5 h: (a) Li:Co = 1.2:1, (b) Li:Co = 1.1:1, and (c) Li:Co = 1.05:1.

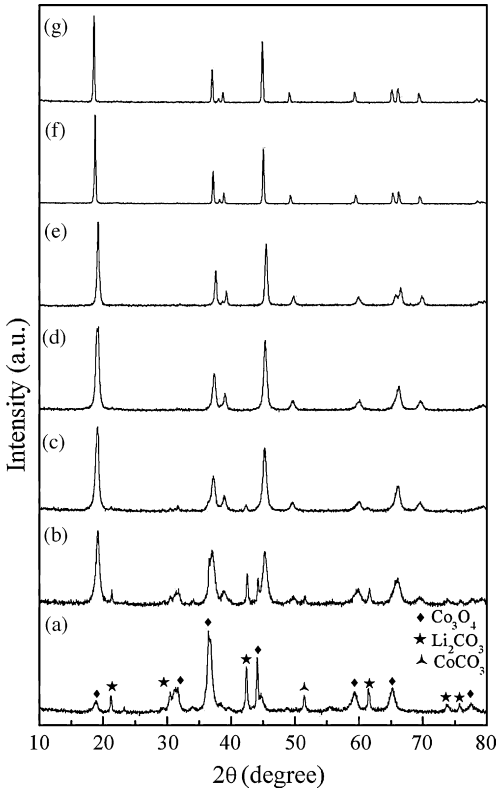

Fig. 3. X-ray diffraction patterns of $LiCoO_2$ powders produced at high temperature heat treatment; Li ratio 1.2: (a) as-deposited powder, (b) 300 °C, (c) 400 °C, (d) 500 °C, (e) 600 °C, (f) 700 °C, and (g) 800 °C.

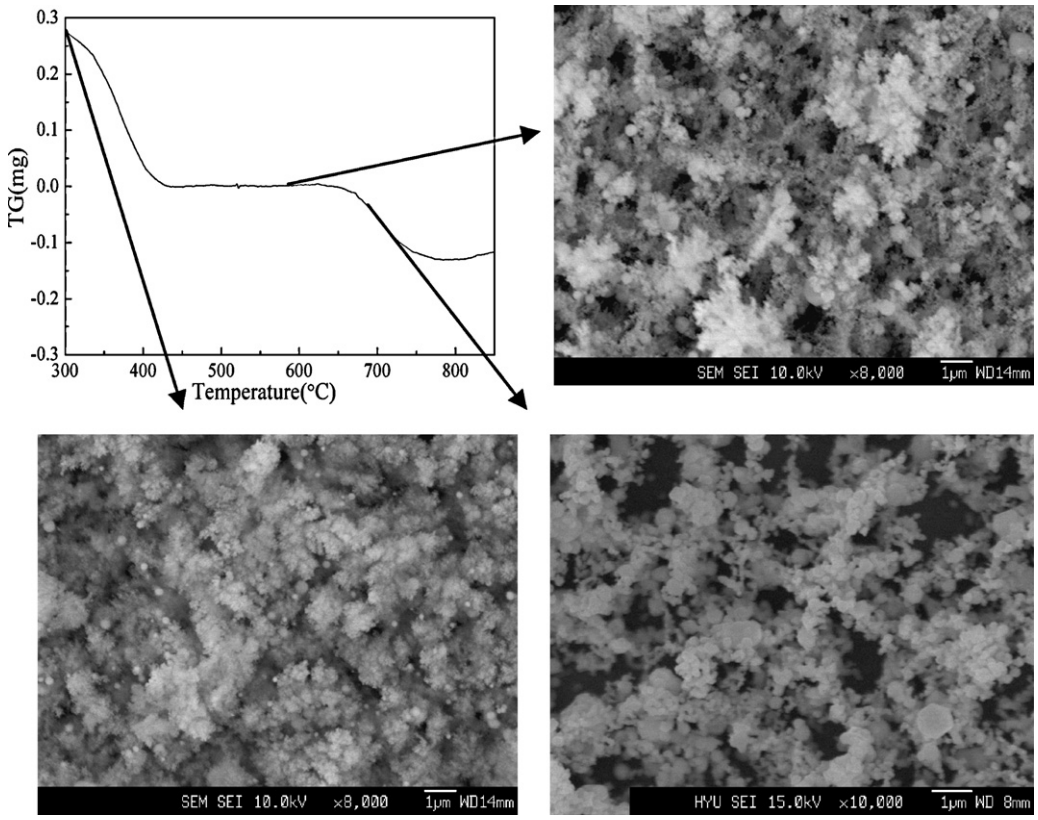

Fig. 4. TG curve of as-deposited powder heated in air and SEM micrographs of deposited soot films at different temperatures.

outer diameter and 133 mm in length), which is made from four concentric silica tubes creating three concentric gaps, and one shield tube keeping flame stable. Argon gas with precursor solution flows through the centermost tube (6 mm outer diameter) of the torch while hydrogen, argon and oxygen flow through three gaps having different width outer diameter (O_2: 12 mm, Ar: 15 mm, and H_2: 21 mm) to ensure laminar flow of gases.

Lithium nitrate ($LiNO_3$) and cobalt acetate tetrahydrate ($Co(CH_3COO)_2{\cdot}4H_2O$) were chosen for starting materials of a precursor solution. The precursor solution of predetermined molar concentration was made by dissolving the starting materials into methyl alcohol (CH_3OH 99.9%). The precursor solution was atomized with an ultrasonic vibrator (1.7 MHz) and the atomized droplets were subsequently carried into the central tube of the torch by flowing dry Ar gas. $LiCoO_2$ were formed by oxy-hydrogen flame and deposited on substrate (Pt plate or silicon) placed in rotating stage, which was kept at 150 °C to eliminate H_2O produced during hydrolysis.

The deposited film and powder composed of synthesized particles is subsequently heat treated or consolidated at the temperature from 300 to 800 °C for 5 h. The $LiCoO_2$ soot powders were synthesized at the hydrogen flow rate of 0.5 l min^{-1}, the oxygen flow rate of 7.5 l min^{-1}, argon shield flow rate of 2.5 l min^{-1}, and solution mole concentration of 0.1 M. The effect of Li/Co ratio was studied by changing the composition of precursor solution.

X-ray diffraction using Cu Kα radiation (XRD, Rigaku M2500) analysis was performed to confirm the crystallinity of the sintered powder and to check the crystalline phases of

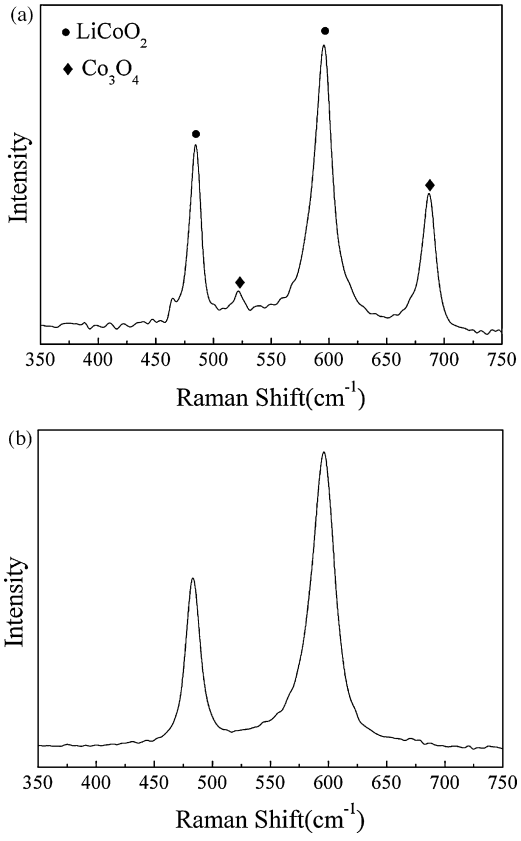

Fig. 5. Raman spectra of $LiCoO_2$ powders sintered at 700 °C produced at different ratio: (a) Li:Co = 1.05:1 and (b) Li:Co = 1.2:1.

$LiCoO_2$ with a scanning step of 0.030° and in the $2\theta/\theta$ range of an angle range from 10° to 80° at scan rate of 3° min^{-1}.

The correlation between the structure and the composition of the $LiCoO_2$ produced by heat treatment was characterized by Raman analysis NRS-3100 JSACO with 514 nm argon laser. To carry out the various measurements, soot powder specimen was used as well as films. Dense bulk specimen was prepared from the soot collected from the deposited films by sintered from 300 to 800 °C. The particles size of $LiCoO_2$ and cross-section of the $LiCoO_2$ thin film were observed by scanning electron microscopy (JEOL, JSM-6330F).

3. Results and discussion

The XRD diffraction patterns of $LiCoO_2$ samples prepared by aerosol flame deposition and sintered at 700 °C for 5 h in air are shown in Fig. 2. Crystalline $LiCoO_2$ has a hexagonal layered structure with the space group *R*-3*m* ($a = 2.82$ Å, $c = 14.08$ Å) in which the cobalt ions locate on the 3a sites of the octahedron, the lithium ions locate on the octahedral 3b spaces and the oxygen anions form cubic close packing [23]. The XRD peaks of the prepared powders in Fig. 2 exhibit that of the layered $LiCoO_2$ phase such as (1 0 1), (1 0 4), (0 1 5), (1 0 7), and (0 1 8) peaks. However, the powder samples in Fig. 2(b and c) with Li molar ratio of 1.05 and 1.1 contained Co_3O_4 as an impurity, which suggests that Li incorporation into the synthesized particle is less efficient than Co. The lower incorporation efficiency of Li is believed to be mainly due to the nebulization efficiency, which would result in the difference in the compositions of the precursor solution and aerosol droplets.

The result indicates that to obtain the phase-pure powder the precursor with at least Li:Co = 1.2:1 is required.

The effect of heat treatment on the synthesized $LiCoO_2$ powder is shown in Fig. 3. As-deposited powder was a mixture of $LiCO_3$, $CoCO_3$, and Co_3O_4. However, as-deposited powder was gradually converted into $LiCoO_2$ as the heat treatment temperature increased. This conversion was not appreciable above 500 °C when judged based on the XRD data shown in Fig. 3. To confirm the reaction route by measuring the thermogravimetric change, TG was measured for the as-deposited powder. Weight loss due to the conversion of carbonates into oxide is known to occur through two mechanisms [23]. The formation of $LiCoO_2$ normally takes one of two routes. The first route is given by the reaction equation;

$$CoCO_3 \rightarrow CoO + CO_2 \quad (1)$$

$$2CoO + Li_2CO_3 + \tfrac{1}{2}O_2 \rightarrow 2LiCoO_2 + CO_2 \quad (2)$$

The second route is given by;

$$3CoCO_3 + \tfrac{1}{2}O_2 \rightarrow Co_3O_4 + 3CO_2 \quad (3)$$

$$2Co_3O_4 + 3Li_2CO_3 + \tfrac{1}{2}O_2 \rightarrow 6LiCoO_2 + 3CO_2 \quad (4)$$

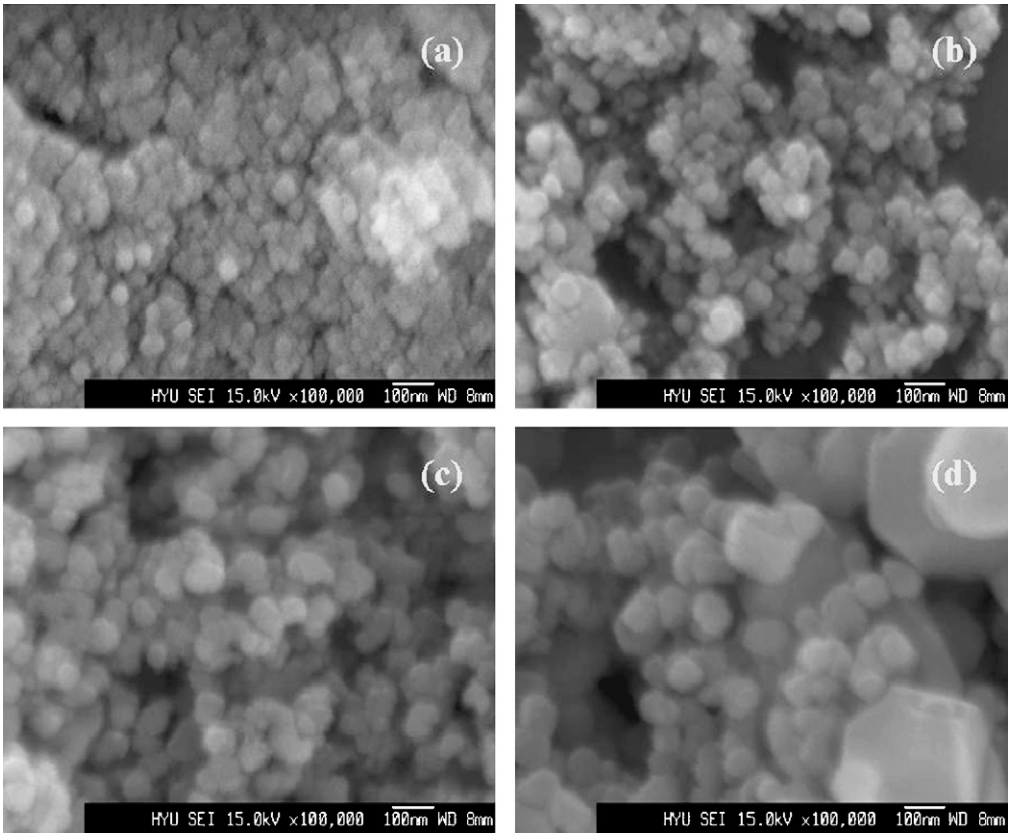

Fig. 6. SEM micrographs showing nano-particles size view of $LiCoO_2$ sintered at different temperatures for 5 h: (a) as-deposited, (b) 500 °C, (c) 600 °C, and (d) 700 °C.

The first reaction route is known to occur under inert atmosphere, while the second one takes place under oxidizing atmosphere such as normal air. As can be seen in Figs. 2 and 3, there was no evidence for the formation of CoO. This speculation is not out of common sense if considering that the heat treatment was done under air in this work. Therefore, we can conclude that the reaction in this work took the second route. It is expected from the reaction Eqs. (3) and (4), one can imagine that the gravimetric curve will show two different drops due to the weight loss of each reactions. The low temperature drop is attributed to the reaction (3) and the high temperature drop is to the reaction (4). In actual powder specimen, the weight loss is highly dependent on the particle size/shape and the packing density since it involves to the evolution of CO_2 gas. The previous reports [23] have shown that the weight loss by the reaction (3) is evident by the precipitous drop in TG graph, while that by the reaction (4) is not evident. The less evident high temperature drop might be due to the large particle size (in the range of μm) used and, maybe, the wide range of reaction temperature of the reaction (4). As shown in Fig. 4, the TG curve measured in this work exhibited two distinct weight losses. The low temperature one occurred around 300 °C, while the high temperature one around 650 °C. It is evident that these two weight losses are assigned to the reactions (3) and (4), respectively. The reason that the high temperature weight loss is very pronounced in this work might be the small particle size in a few tens of nanometers scale and very low packing density of the prepared specimen as shown in the inset figures. The significant weight loss around 650 °C can be clearly seen in the inset figure, which supports the observation by TG measurement. If judging from the TG result, the optimum calcinations temperature of the synthesized powder will be around 750 °C where the weight loss due to CO_2 gas evolution is completed. However, as explained later, the cation mixing is another factor to consider determining the optimum calcinations temperature.

In Fig. 3, the peaks at $2\theta = 65°$ were not clearly separated when the powder was sintered under 600 °C. When the sintering temperature is higher than 600 °C, the XRD patterns show the characteristic of fine-layered $LiCoO_2$. All diffraction peaks could be indexed to the hexagonal α-$NaFeO_2$ (*R*-3*m*) lattice structure. From peak positions the lattice constants of the samples were calculated as listed in Table 1. The *c*-axis and the *c*/*a* ratio increase with the increase of sintering temperature, while *a*-axis changes slightly. In Table 1, *R* is the ratio of the intensity of (0 0 3) peak to (1 0 4) peak and at the temperatures above 500 °C *R* is higher than 1.2, which suggests that the cation mixing was eliminated in satisfactory level [24]. The FWHMs of the peaks were obviously reduced and their intensity increased as the sintering temperature increased, which is the result of improved crystallinity. However, the *R* ratio was reduced for the powder specimen sintered at 800 °C, which coincides with the previous reports [24,25].

Table 1
The lattice parameters of $LiCoO_2$ heat treated at various temperatures

Temperature (°C)	*R*	*a* (Å)	*c* (Å)	*c*/*a*
500	1.18	2.818	13.865	4.920
600	1.32	2.806	13.986	4.984
700	1.59	2.820	14.090	4.996
800	1.39	2.826	14.136	5.002

Fig. 5 shows the Raman spectra of $LiCoO_2$ samples with different Li ratio (1.2 and 1.05) which were sintered at 700 °C for 5 h in air. The Raman peaks at 484 and 594 cm^{-1} were observed in the both samples and these peaks are assigned as E_g and A_{1g} vibration modes in hexagonal *R*-3*m* space group of $LiCoO_2$, respectively.

In the Raman spectrum of Fig. 5(a), an impurity peak assigned to Co_3O_4 was observed at 521 and 686 cm^{-1} while the bands assigned to Li_2CO_3 were not observed [26]. This result agrees to the result of XRD diffraction patterns shown in Fig. 2(c).

The micrographs of $LiCoO_2$ samples sintered at various temperatures from as-deposited to 700 °C were taken by SEM and displayed in Fig. 6. The particle size distribution was relatively narrow and the shape was close to a sphere. The average particle size of the powder increased with the increasing of sintering temperature. For the samples as-deposited and sintered at 500, 600, and 700 °C the particle sizes are in the range of 30–40, 40–50, 50–60, and 60–70 nm, respectively.

The cross-sectional images of as-deposited and sintered film are shown in Fig. 7. The thickness of $LiCoO_2$ film before the

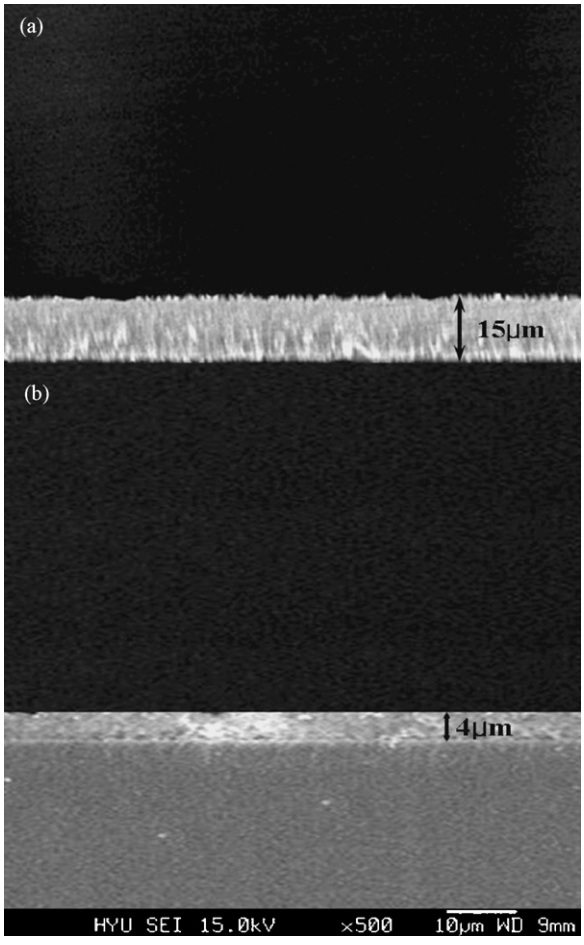

Fig. 7. SEM micrograph showing cross-sectional view of $LiCoO_2$ (a) as-deposited and (b) sintered at 700 °C for 5 h.

consolidation process was about 15 μm and it reduced to 4 μm after sintering. The film retained the partially porous state even after sintering process at 700 °C for 5 h, which is expected to be desirable for 3-D contact with solid-state electrolyte.

4. Conclusions

The crystalline $LiCoO_2$ nano-particles were synthesized by the aerosol flame deposition from the aqueous solution of lithium nitrate ($LiNO_3$) and cobalt acetate tetrahydrate ($Co(CH_3COO)_2{\cdot}4H_2O$). The as-synthesized powder composed of various compounds such as Li_2CO_3, Co_3O_4, and $CoCO_3$. Subsequent sintering process at 700 °C, for about 5 h produced crystalline $LiCoO_2$ nano-particles without cation mixing. The average particle size of $LiCoO_2$ was under 70 nm and increase with the increase of heat treatment temperature. $LiCoO_2$ soot film of 15 μm thickness was consolidated to 4 μm after sintering at 700 °C for 5 h.

In this work, aerosol flame deposition method was successfully applied to the fabrication of $LiCoO_2$ nano-powder and film for thin film battery and proved its potential as a candidate for inexpensive fabrication process.

Acknowledgement

This work was supported by the Ministry of Information & Communications, Korea, under the Information Technology Research Center (ITRC) Support Program.

References

[1] N.J. Dudney, Mater. Sci. Eng. B116 (2005) 245.
[2] N. Kuwata, J. Kawamura, K. Toribami, T. Hattori, N. Sata, Electrochem. Commun. 6 (2004) 417.
[3] C. Julien, A. Gorenstein, Ionics 1 (1995) 193.
[4] C. Julien, B. Yebka, J.P. Guesdon, Ionics 1 (1995) 316.
[5] P. Birke, W.F. Chu, W. Weppner, Solid State Ionics 93 (1997) 1.
[6] S.P. Sheu, C.Y. Yao, J.M. Chen, Y.C. Chiou, J. Power Sources 68 (1997) 533–535.
[7] K. Mizushima, P.C. Jones, P.C. Wiseman, J.B. Goodenough, Mater. Res. Bull. 15 (1980) 783.
[8] T. Nagaura, K. Tozawa, Progr. Batt. Solar Cells 9 (1991) 209.
[9] M. Antaya, J.R. Dahn, J.S. Preston, E. Rossen, J.N. Reimers, J. Electrochem. Soc. 140 (1993) 575.
[10] P. Fragnaud, T. Brousse, D.M. Schleich, J. Power Sources 63 (1996) 187.
[11] B. Wang, J.B. Bates, F.X. Hart, B.C. Sales, R.A. Zuhr, J.D. Robertson, J. Electrochem. Soc. 143 (1996) 3203.
[12] G. Wei, T.E. Hass, R.B. Goldner, Solid State Ionics 58 (1992) 115.
[13] R.B. Goldner, S. Slaven, T.Y. Liu, T.E. Haas, F.O. Arntz, P. Zerigian, Mater. Res. Soc. Symp. Proc. 369 (1995) 137.
[14] K. Kanamura, S. Toriyama, S. Shiraishi, M. Ohashi, Z. Takehara, J. Electroanal. Chem. 419 (1996) 77.
[15] J.B. Bates, N.J. Dudney, B. Neudecker, A. Ueda, C.D. Evans, Proceedings of 12th International Conference on Solid State Ionics, vol. 6, 1999.
[16] J.K. Lee, S.J. Lee, H.K. Baik, H.Y. Lee, S.W. Jang, S.M. Lee, Electrochem. Solid-State Lett. 2 (1999) 512.
[17] C. Chen, E.M. Kelder, P.J.J.M. van der Put, J. Schoonman, J. Mater. Chem. 6 (1996) 765.
[18] K. Yamada, N. Sato, T. Fujino, C.G. Lee, I. Uchida, J.R. Selman, J. Solid-State Electochem. 3 (1999) 148.
[19] I. Uchida, H. Sato, J. Electrochem. Soc. 142 (1995) L139.
[20] K.A. Striebel, C.Z. Deng, S.J. Wen, E.J. Cairns, J. Electrochem. Soc. 143 (1996) 1821.
[21] J.G. Zhang, J.M. McGraw, J. Turner, D. Ginley, J. Electrochem. Soc. 144 (1997) 1630.
[22] Y. Wang, Q.Z. Qin, J. Electrochem. Soc. 149 (2002) A873.
[23] A. Lundblad, B. Bergman, Solid State Ionics 96 (1997) 173.
[24] S.T. Myung, N. Kumagai, S. Komaba, H.-T. Chung, J. Appl. Electrochem. 30 (2000) 1081.
[25] Q. Wu, W. Li, Y. Cheng, Z. Jiang, Mater. Chem. Phys. 91 (2005) 463.
[26] M. Inaba, Y. Iriyama, Z. Ogumi, Y. Todzuka, A. Tasaka, J. Raman Spectrosc. 28 (1997) 613.